



Molecular Crystals and Liquid Crystals

Publication details, including instructions for authors and subscription information:

<http://www.tandfonline.com/loi/gmcl20>

Synthesis and Mesomorphic Properties of 2-(4-Alkyloxyphenyl)benzothiazoles

Sie-Tiong Ha^a, Teck-Ming Koh^a, Guan-Yeow Yeap^b,
Hong-Cheu Lin^c, Peng-Lim Boey^b, Yip-Foo Win^a,
Siew-Teng Ong^a & Lay-Khoon Ong^a

^a Faculty of Engineering and Science, Universiti Tunku Abdul Rahman, Jalan Genting Klang, Setapak, Kuala Lumpur, Malaysia

^b Liquid Crystal Research Laboratory, School of Chemical Sciences, Universiti Sains Malaysia, Minden, Penang, Malaysia

^c Department of Materials Science and Engineering, National Chiao Tung University, Hsinchu, Taiwan, China

Published online: 03 Aug 2009.

To cite this article: Sie-Tiong Ha, Teck-Ming Koh, Guan-Yeow Yeap, Hong-Cheu Lin, Peng-Lim Boey, Yip-Foo Win, Siew-Teng Ong & Lay-Khoon Ong (2009) Synthesis and Mesomorphic Properties of 2-(4-Alkyloxyphenyl)benzothiazoles, *Molecular Crystals and Liquid Crystals*, 506:1, 56-70, DOI: [10.1080/15421400902987347](https://doi.org/10.1080/15421400902987347)

To link to this article: <http://dx.doi.org/10.1080/15421400902987347>

PLEASE SCROLL DOWN FOR ARTICLE

Taylor & Francis makes every effort to ensure the accuracy of all the information (the "Content") contained in the publications on our platform. However, Taylor & Francis, our agents, and our licensors make no

representations or warranties whatsoever as to the accuracy, completeness, or suitability for any purpose of the Content. Any opinions and views expressed in this publication are the opinions and views of the authors, and are not the views of or endorsed by Taylor & Francis. The accuracy of the Content should not be relied upon and should be independently verified with primary sources of information. Taylor and Francis shall not be liable for any losses, actions, claims, proceedings, demands, costs, expenses, damages, and other liabilities whatsoever or howsoever caused arising directly or indirectly in connection with, in relation to or arising out of the use of the Content.

This article may be used for research, teaching, and private study purposes. Any substantial or systematic reproduction, redistribution, reselling, loan, sub-licensing, systematic supply, or distribution in any form to anyone is expressly forbidden. Terms & Conditions of access and use can be found at <http://www.tandfonline.com/page/terms-and-conditions>

Synthesis and Mesomorphic Properties of 2-(4-Alkyloxyphenyl)benzothiazoles

Sie-Tiong Ha¹, Teck-Ming Koh¹, Guan-Yeow Yeap²,
Hong-Cheu Lin³, Peng-Lim Boey², Yip-Foo Win¹,
Siew-Teng Ong¹, and Lay-Khoon Ong¹

¹Faculty of Engineering and Science, Universiti Tunku Abdul Rahman,
Jalan Genting Klang, Setapak, Kuala Lumpur, Malaysia

²Liquid Crystal Research Laboratory, School of Chemical Sciences,
Universiti Sains Malaysia, Minden, Penang, Malaysia

³Department of Materials Science and Engineering, National Chiao
Tung University, Hsinchu, Taiwan, China

A homologous series of 2-(4-alkyloxyphenyl)benzothiazoles with an even number of carbons in the terminal alkoxy chain was synthesized and characterized. The structure of the compounds was postulated using elemental analyses, FT-IR, NMR, and mass spectrometry techniques. Their liquid crystalline properties have been investigated by optical polarizing microscopy, DSC, and X-ray diffraction (XRD) techniques. Whilst the n-octyloxy to n-hexadecyloxy derivatives exhibited a monotropic smectic A phase, the n-ethoxy to n-hexyloxy and the n-octadecyloxy derivatives were not mesogenic. The mesomorphic properties of the present series were compared with other structurally related series to establish the chemical structure-mesomorphic properties relationship.

Keywords: 2-(4-alkyloxyphenyl)benzothiazole; heterocycles; Smectic A; structure-property relationship

INTRODUCTION

Conventional thermotropic liquid crystals consist of anisotropic molecules that are either rod-shaped (calamitic) or disc-shaped (discotic) [1]. The 1,4-disubstituted phenyl rings forms the linear core in majority of the low molar mass calamitic mesogen systems. Over the

Address correspondence to Sie-Tiong Ha, Faculty of Engineering and Science, University Tunku Abdul Rahman, Jalan Genting Klang, Setapak, Kuala Lumpur 53300, Malaysia. E-mail: hast@utar.edu.my

past few decades, liquid crystals comprising heterocycles as core units have received overwhelming attention due to their unique properties [2–4]. Earlier report has shown that the introduction of heterocycles as the central core has greatly influenced the mesomorphic properties of the calamatic molecules owing to their unsaturation and/or their more polarizable nature [5]. It has also been claimed that the inclusion of the heteroatom considerably changes the polarity, polarizability, and to a certain extent the geometry of the molecule, thereby influencing the type of mesophase, the phase transition temperatures, dielectric constants, and other properties of the mesogens [6,7].

The slightly bent structure of mesogen possessing a single heterocyclic ring such as thiophene has led to unique physical properties such as reduced packing ability, medium to strong lateral dipole, high anisotropy of polarizability and low viscosity. Materials consisting of thiophene, 1,3-thiazole, or 1,3,4-thiadiazole as the core unit have significant lateral dipole moments which would contribute to physical parameters such as increased dielectric anisotropy and dielectric biaxiality [2]. Other examples of single heterocyclic ring liquid crystals include those with furyl [8], pyridine [8–10], substituted pyrimidine carboxylic acid [11], thiazole [12], thiadiazole [13], and oxadiazole [14] moieties.

Benzothiazole, another type of heterocycle, has emerged in its usage as a core unit in calamitic liquid crystals. It has been reported that liquid crystalline compounds incorporating a benzothiazole-fused ring exhibit good hole-transporting properties with a low ionization potential, making them of potential interest as hole-transporting materials in organic light-emitting devices (OLEDs) [15–17]. Pavluchenko *et al.* [18] reported on mesogens comprising benzothiazole and benzoxazole with central linkages and lateral substituents at different positions so as to evaluate the effect of structural changes on mesomorphic properties. Substitution at the sixth position of the benzothiazole ring was found to be thermally more stable as compared to that of the fifth position. Belmar *et al.* [19] studied the influence of central linking groups on the mesomorphic properties of 6-*n*-decyloxy-2-(4-alkoxybenzylidene-amino)benzothiazoles, *n*-[2-(6-*n*-decyloxybenzothiazolyl)]-4-*n*-alkoxybenzamides, and 6-*n*-decyloxy-2-(4-*n*-alkoxyphenylazo)benzothiazoles. Results indicated that the imine and azo derivatives both exhibited smectic and nematic phases while only the smectic phase was observed for the amide derivatives. This observation can be ascribed to the hydrogen bonding between the molecules of the amide derivatives, which prevent the formation of nematic phase [19].

Prajapati and Bonde reported two mesogenic homologous series comprising 6-substituted-benzothiazole ring systems with an azo

centre linkage [20]. The study revealed that the methoxyl substituent at the sixth position of the benzothiazole ring favored the formation of the nematic phase. As part of our studies on heterocyclic mesogens, we report in this article the synthesis and the mesomorphic properties of a homologous series of 2-(4-alkyloxyphenyl)benzothiazoles without central linking groups and lateral substituents. In addition, they were compared to structurally related compounds to establish the chemical structure-mesomorphic properties relationship.

EXPERIMENTAL

2-Aminothiophenol, 1-bromoalkane ($C_nH_{2n+1}Br$ where $n = 2, 4, 6, 8, 10, 12, 14, 16, 18$), and potassium iodide were obtained from Merck (Germany). 4-Hydroxybenzaldehyde was purchased from Acros Organics (USA). Potassium hydroxide was obtained from R&M Chemicals (U.K.).

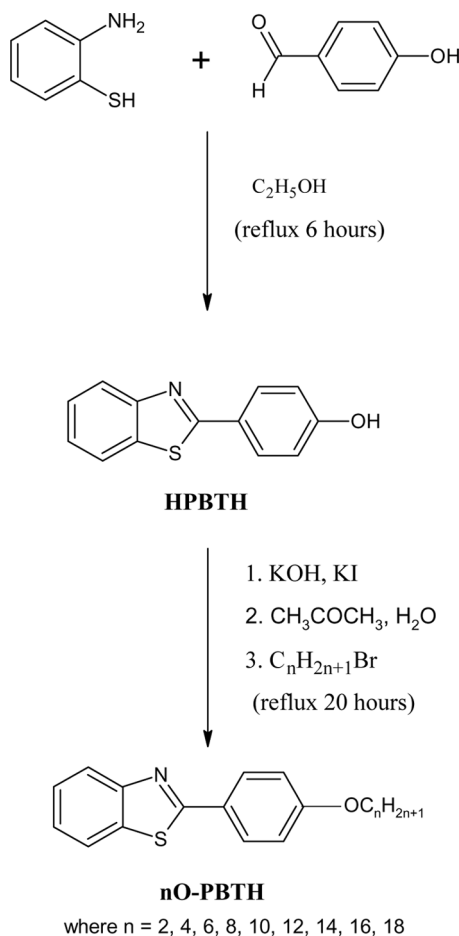
IR spectra were recorded using a Perkin-Elmer System 2000 FT-IR Spectrometer via KBr disc procedure. The range of measurement was from $4000\text{--}400\text{ cm}^{-1}$. 1H NMR (400 MHz) and ^{13}C NMR (100 MHz) spectra were recorded in $CDCl_3$ using a Bruker Avance 400 MHz Spectrometer with TMS as the internal standard. EI-MS (70 eV) were measured with a Mass Spectrometer Finnigan MAT95XL-T at a source temperature of $200^\circ C$. The sample was introduced using direct inlet probe. Microanalyses were carried out on Perkin Elmer 2400 LS Series CHNS/O analyzer. Melting points of the synthesized compounds were determined using a Barnstead Electrothermal Melting Point Apparatus. Thin Layer Chromatography (TLC) was carried out on aluminium-backed silica-gel plates (Merck 60 F₂₅₄) and visualized under short-wave UV light.

Phase-transition temperatures and enthalpy changes were measured using a Differential Scanning Calorimeter Mettler Toledo DSC823^e at heating and cooling rates of $10^\circ C/min$ and $-10^\circ C/min$, respectively. A polarizing optical microscope (Carl Zeiss) equipped with a Linkam heating stage was used for temperature dependent studies of the liquid crystal textures. A video camera (Video Master coomo20P) installed on the polarizing microscope was coupled to a video capture card (Video Master coomo600), allowing real-time video capture and image saving. Textures exhibited by the compounds were observed using polarized light with crossed polarizers. Samples were prepared as thin films sandwiched between a glass slide and a cover slip. Phase identification was made by comparing the observed textures with those reported in the literature [21,22].

Synchrotron powder X-ray diffraction (XRD) measurements were performed at beamline BL17A of the National Synchrotron Radiation

Research Center (NSRRC) in Taiwan, where the X-ray wavelength used was 1.32633 \AA . XRD data were collected using imaging plates (IP, of an area $= 20 \times 40 \text{ cm}^2$ and a pixel resolution of 100) curved with a radius equivalent to the sample-to-image plate distance of 280 mm, and the diffraction signals were accumulated for 3 min. The powder samples were packed into a capillary tube and heated by a heat gun, where the temperature controller is programmable by a PC with a PID feedback system. The scattering angle theta was calibrated by a mixture of silver behenate and silicon.

The synthetic route of 2-(4-alkyloxyphenyl)benzothiazoles, **nO-PBTH** is illustrated in Scheme 1.



SCHEME 1 Synthetic route of **nO-PBTH**.

Synthesis

Synthesis of 2-(4-Hydroxyphenyl)benzothiazole, HPBTH

The compound was synthesized according to the method described by Toba *et al.* [23]. Five mmol (0.6260 g) of 2-aminothiophenol and 5 mmol (0.6106 g) of 4-hydroxybenzaldehyde were refluxed upon stirring for 6 hours in 40 mL of ethanol. The reaction mixture was subsequently cooled to room temperature following which to it 60 mL of distilled water was added slowly until the mixture turned cloudy. It was refrigerated overnight at about 20°C, and the solid formed was filtered and washed with cold ethanol:water (1:1.5) and dichloromethane. Yield 75%. IR (KBr) ν_{\max} cm⁻¹ 3417 (O-H), 3053, 2996 (C-H aromatic), 1606 (C=N, thiazole), 1483, 1455 (C=C aromatic), 1074 (C-S-C). ¹H NMR (400 MHz, CDCl₃): δ /ppm 5.3 (1 H, s, OH), 6.9 (2 H, d, Ar-H), 7.3 (1 H, t, Ar-H), 7.4 (1 H, t, Ar-H), 7.9 (1 H, d, Ar-H), 8.0 (3 H, m, Ar-H).

Synthesis of 2-(4-Alkyloxyphenyl)benzothiazoles, nO-PBTH

2-(4-Alkyloxyphenyl)benzothiazoles were synthesized via modification of the method described by Prajapati *et al.* [24]; 0.9 mmoles (0.2046 g) of HPBTH in 35 ml of acetone and 0.9 mmoles (0.0505 g) of KOH in 5 ml of distilled water were mixed in a round bottom flask to which a small amount of KI was added as a catalyst. The mixture was refluxed upon stirring for 1 hour following which 1.35 mmoles of the appropriate 1-bromoalkane (C_nH_{2n+1}Br, n = 2, 4, 6, 8, 10, 12, 14, 16, 18) was added and was further refluxed for another 20 hours. The mixture was cooled to room temperature, and the white precipitate formed was separated by filtration. The solid obtained was recrystallized several times with absolute ethanol whereupon the pure compound was isolated. The percentage yields and analytical data of the title compounds are tabulated in Table 1. The IR, NMR (¹H and ¹³C), and mass spectral data for the representative compound, 16O-PBTH, are summarized as follows.

16O-PBTH: Yield 63%. IR (KBr) ν_{\max} cm⁻¹ 3057, 3030 (C-H aromatic), 2955, 2849 (C-H aliphatic), 1608 (C=N, thiazole), 1487, 1465 (C=C aromatic), 1261 (Ar-O-R ether), 1073 (C-S-C, thiazole). ¹H NMR (400 MHz, CDCl₃): δ /ppm 0.9 (t, 3 H, CH₃-), 1.3–1.5 (m, 26 H, CH₃-(CH₂)₁₃-CH₂-CH₂-O-), 1.8–1.9 (m, 2 H, -CH₂-CH₂-O-), 4.1 (t, 2H, -CH₂-O-), 7.0 (d, 2 H, Ar-H), 7.4 (t, 1 H, Ar-H), 7.5 (t, 1 H, Ar-H), 7.9 (d, 1 H, Ar-H), 8.0 (m, 3 H, Ar-H). ¹³C NMR (100 MHz, CDCl₃): δ /ppm 168.44 (C=N), 161.96, 154.59, 135.21, 129.49, 126.62, 126.50, 125.18, 123.17, 121.93, 115.24 for aromatic carbons, 68.64 (-O-CH₂-), 32.38, 30.16, 30.14, 30.12, 30.05, 30.02, 29.83, 29.60, 26.44, 23.15 for methylene carbons [- (CH₂)₁₄CH₂O-], 14.61 (-CH₃). EI-MS m/z (rel. int. %): 451(42) (M)⁺, 227(100).

TABLE 1 Percentage Yields and Analytical Data of **nO-PBTH**

Compound	Yield (%)	Formula	% Found (% Calcd.)		
			C	H	N
2O-PBTH	37	C ₁₅ H ₃₁ NOS	70.50 (70.56)	5.19 (5.13)	5.43 (5.49)
4O-PBTH	49	C ₁₇ H ₁₇ NOS	72.09 (72.05)	6.11 (6.05)	4.89 (4.94)
6O-PBTH	43	C ₁₉ H ₂₁ NOS	73.29 (73.31)	6.80 (6.75)	4.45 (4.50)
8O-PBTH	43	C ₂₁ H ₂₅ NOS	74.36 (74.34)	7.51 (7.37)	3.95 (4.13)
10O-PBTH	47	C ₂₃ H ₂₉ NOS	75.22 (75.20)	8.08 (7.90)	3.70 (3.81)
12O-PBTH	44	C ₂₅ H ₃₃ NOS	75.90 (75.95)	8.43 (8.35)	3.63 (3.54)
14O-PBTH	52	C ₂₇ H ₃₇ NOS	76.58 (76.60)	8.87 (8.75)	3.17 (3.31)
16O-PBTH	63	C ₂₉ H ₄₁ NOS	77.13 (77.16)	9.18 (9.09)	3.18 (3.10)
18O-PBTH	71	C ₃₁ H ₄₅ NOS	77.53 (77.66)	9.52 (9.39)	2.83 (2.92)

RESULTS AND DISCUSSION

Structural identification of the title compounds was carried out by employing a combination of elemental analysis and spectroscopic techniques (FT-IR, NMR, and EI-MS). The percentages of C, H, and N from the elemental analysis conform with the calculated values for compounds **nO-PBTH** (where $n = 2, 4, 6, 8, 10, 12, 14, 16, 18$) and are presented in Table 1. The prominent molecular ion peak at m/z 451 in the mass spectrum of **16O-PBTH**, establishing a molecular formula of C₂₉H₄₁ONS, which supports the proposed structure.

FTIR, ¹H NMR, and ¹³C NMR Spectral Studies

The diagnostic absorption bands at 2849 and 2955 cm⁻¹ in the FTIR spectrum of **16O-PBTH** provides evidence for the alkoxy chain. The presence of the aromatic rings was inferred from the absorption bands at 3030, 3057, 1487, and 1465 cm⁻¹. The absorption bands assignable to the stretching of the C=N and C-S-C bonds of benzothiazole were observed at 1608 and 1073 cm⁻¹, respectively. These values conform with those reported in the IR spectra for various substituted benzothiazoles [20,25]. The absorption band at 1261 cm⁻¹ was indicative of the C-O stretching of the aromatic ether (Ar-O-R). Compounds **nO-PBTH** ($n = 2, 4, 6, 8, 10, 12, 14, 18$) exhibited similar characteristic absorptions as discussed for **16O-PBTH**.

The triplets at $\delta = 0.9$ and 4.1 ppm in the ¹H NMR spectrum of **16O-PBTH** were assigned to methyl protons and methylene protons (Ar-O-CH₂-) that bonded directly to aromatic ether group, respectively. The multiplets between $\delta = 1.3$ –1.9 ppm were attributed to the remaining methylene protons [CH₃-(CH₂)₁₄-] of the alkoxy chain.

The ^1H NMR spectrum of **160-PBTH** also suggests the presence of eight aromatic protons.

The ^{13}C NMR spectrum of **160-PBTH** suggests the presence of 29 carbons. The peak at $\delta = 168.44$ ppm owing to the presence of the imine carbon ($-\text{C}=\text{N}-$, thiazole), was in agreement with that reported in literature [19]. The signals within the range of $\delta = 115.24$ – 161.96 ppm were assigned to the carbons of the benzothiazole and aromatic moieties. The carbon resonances between $\delta = 14.61$ – 68.64 ppm were indicative of the methylene and methyl carbons of the alkoxy chain. The results as inferred from the IR and NMR spectral data of the title compounds were consistent with the proposed structure.

Phase-Transition Behavior and Liquid Crystallinity of **nO-PBTH**

The transition temperatures and associated enthalpy changes of **nO-PBTH** obtained from the DSC measurements are summarized in Table 2. The DSC thermograms of all the members during the heating and cooling cycles are depicted in Figures 1 and 2, respectively. The representative optical photomicrographs are shown in Figure 3. A plot of the transition temperatures against the number of carbons

TABLE 2 Transition Temperatures and Associated Enthalpy Changes of **nO-PBTH** Upon Heating and Cooling

Compound	Transition temperatures, °C (ΔH , kJ mol $^{-1}$)
20-PBTH	Cr 125.7 (18.18) I
	<i>Cr 95.7 (16.16) I</i>
40-PBTH	Cr 89.5 (36.16) I
	<i>Cr 78.0 (34.71) I</i>
60-PBTH	Cr 85.1 (20.87) I
	<i>Cr 73.0 (20.12) I</i>
80-PBTH	Cr 75.5 (27.86) I
	<i>Cr 48.8 (17.12) SmA 74.8 (6.97) I</i>
100-PBTH	Cr 81.7 (44.42) I
	<i>Cr 63.1 (32.03) SmA 79.3 (8.80) I</i>
120-PBTH	Cr 86.9 (55.61) I
	<i>Cr 63.8 (42.11) SmA 81.2 (10.41) I</i>
140-PBTH	Cr 91.7 (59.52) I
	<i>Cr 70.7 (47.00) SmA 81.2 (9.79) I</i>
160-PBTH	Cr 95.7 (70.41) I
	<i>Cr 77.3 (57.37) SmA 79.8 (11.20) I</i>
180-PBTH	Cr 96.8 (58.49) I
	<i>Cr 85.2 (56.27) I</i>

The values in *italics* were taken during cooling cycle.

Cr = Crystal; SmA = Smectic A; I = Isotropic liquid.

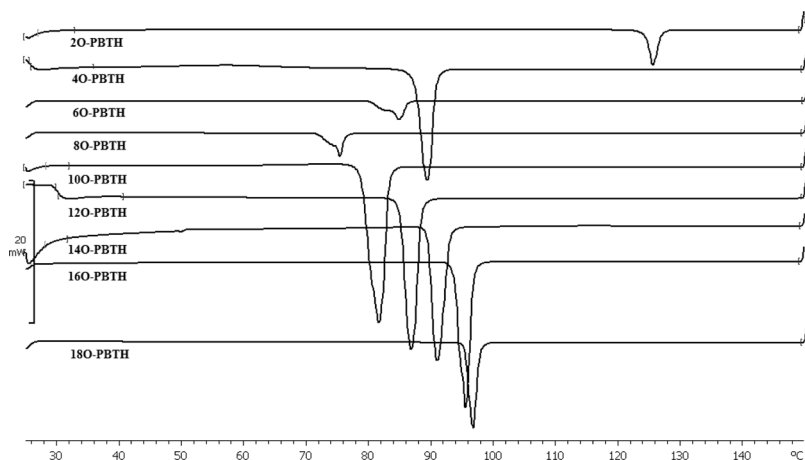


FIGURE 1 DSC thermograms of **nO-PBTH** during heating cycle.

in the alkoxy chain during the heating and cooling cycles are shown in Figures 4 and 5. Based on the plot, it can be deduced that the meso-phase behaviors were greatly influenced by the length of the terminal chains. The crystal-isotropic transition (melting) temperatures exhibited a descending trend as the length of the terminal alkoxy chain of the derivatives increased from C2 to C8. However, the lengthening of carbon chain from the n-octyloxy to the n-octadecyloxy derivatives led to ascending trend of melting temperatures. This phenomenon can be

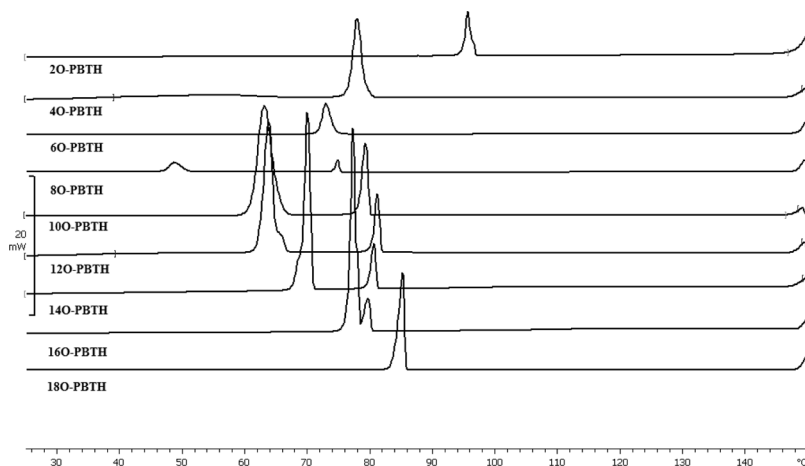
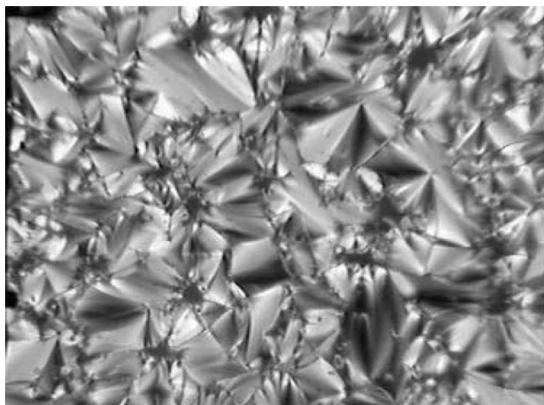
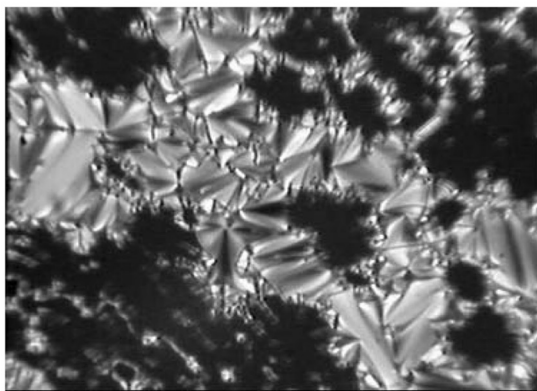


FIGURE 2 DSC thermograms of **nO-PBTH** during cooling cycle.



(a)



(b)

FIGURE 3 (a) Optical photomicrograph of **100-PBTH** exhibiting homogeneously aligned smectic A phase with fan-shaped textures; (b) optical photomicrograph of **120-PBTH** exhibiting smectic A phase with fan-shaped and homeotropic (dark area) textures.

attributed to the the increased intermolecular Van der Waals attraction as the length of the alkoxy chain increased [26].

Under the polarizing microscope, the n-octyloxy to the n-hexadecyloxy derivatives exhibited monotropic smectic A phase. In the monotropic mesogens, the melting points were always equal to or higher than the clearing points, hence exhibiting supercooling properties [27]. As a representative illustration, the optical photomicrographs of compounds **100-PBTH** and **120-PBTH** are illustrated in Fig. 3. **100-PBTH** exhibited homogenously aligned fan-shaped

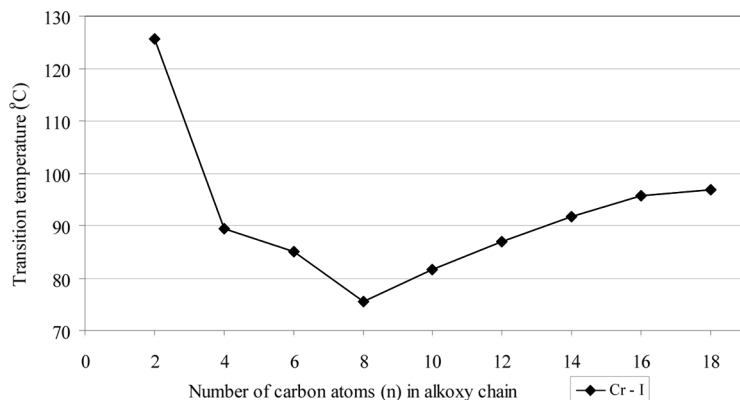


FIGURE 4 Plot of transition temperatures versus the number of carbons (n) in the alkoxy chain of **nO-PBTH** during heating cycle.

textures whereas the co-existence of homogenous and homeotropic (dark region) smectic A with fan-shaped textures were observed for **12O-PBTH**. The assignments of the mesophases were made on the basis of the textures observed from POM as the mesophases displayed the typical fan-shaped textures for a smectic A phase [21,22].

The rest of the members ($n=2, 4, 6$, and 18) did not exhibit liquid crystal phases. **2O-PBTH**, **4O-PBTH**, and **6O-PBTH** were

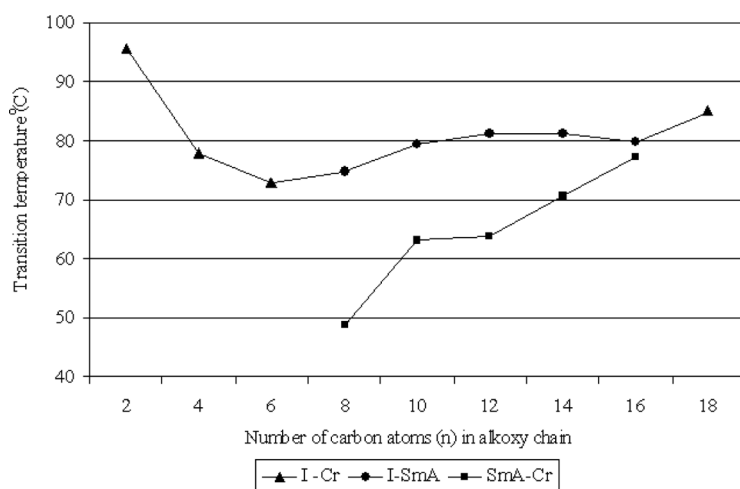


FIGURE 5 Plot of transition temperatures versus the number of carbons (n) in the alkoxy chain of **nO-PBTH** during cooling cycle.

non-mesomorphic perhaps due to the shorter terminal alkoxy chains, resulting in higher melting points, thus suppressing the liquid crystal phase. The high flexibility owing to the long terminal chain ($C_{18}H_{36}O-$) in **180-PBTH** also depressed the formation of liquid crystal phase [28].

XRD Studies of *nO*-PBTH

Although the liquid crystal phase type of the title compound can be concluded preliminary by DSC and POM, it is necessary to measure them by XRD analysis and give additional information about their structure parameters. XRD patterns of representative compounds **100-PBTH** and **120-PBTH** are shown in Fig. 6.

In general, a smectic, nematic, cholesteric structure has a broad peak associated with lateral packing at $2\theta \approx 16$ – 21° in a wide-angle XRD curve. A sharp and strong peak at a low angle ($1^\circ < 2\theta < 6^\circ$) in a small angle X-ray scattering curve can be observed for smectic structures, but it cannot be seen for nematic and cholesteric structures [29–31]. An XRD pattern of **100-PBTH** and **120-PBTH** showed sharp reflection peaks at 2θ of 2.99 and 2.65 ($d = 25.56$ and 28.84 Å), which were corresponding to the smectic layer spacing. Combining the polarized microscopy with XRD measurements confirmed that these compounds were smectogenic A.

Chemical Structure–Mesomorphic Property Relationship

There is a close relationship between the mesomorphic properties and molecular structure of organic compounds. Thus, transition temperatures, mesophase range, and types of mesophases can be correlated with the molecular structure of the compounds. In Table 3, the transition temperatures, types of mesophases, mesophase range, and molecular structure of **80-PBTH** are compared with other structurally related compounds **A** [20], **B** [32], and **C** [19].

Whilst **80-PBTH** exhibited a smectic A phase, compound **A** was nematogenic. The difference could be resulted from the additional methoxyl group at the sixth position of the benzothiazole ring along with the additional azo linkage between the two aromatic rings in compound **A**. Hence, the nematic phase in compound **A** could be due to the methoxyl substituent which diminished the formation of the smectic A [9]. The azo linkage between the two aromatic core units in compound **A** conferred stepped core structure leading to the broadening effect, thus disrupting the lamellar packing, and therefore generating the nematic phase [1]. Similar structure–property relationship was also inferred from compound **C** whereby this structurally related compound exhibited a nematic phase owing to the presence of an azo linkage.

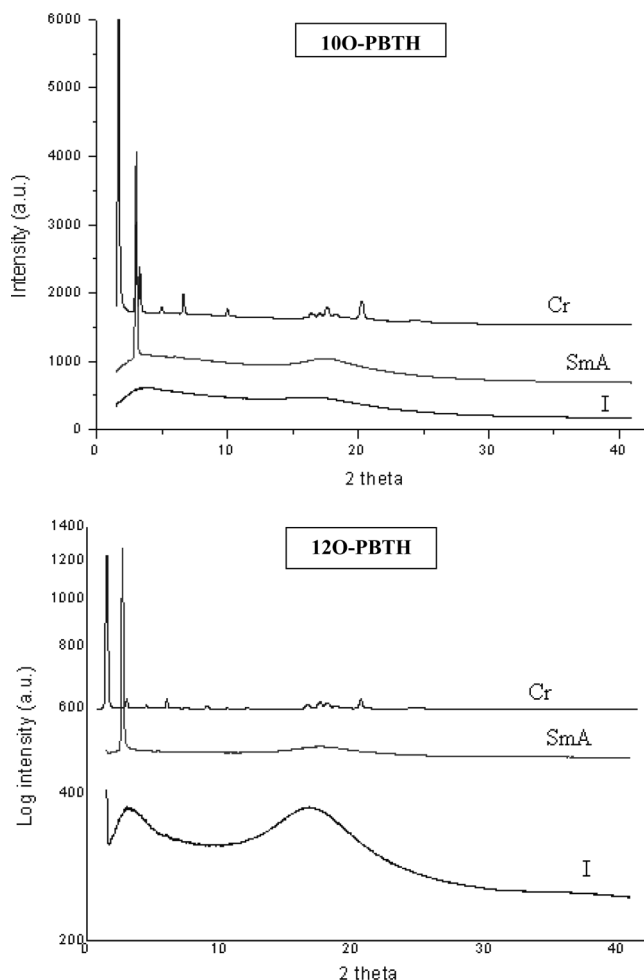
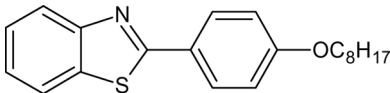
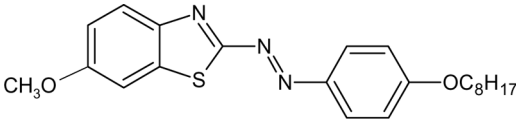
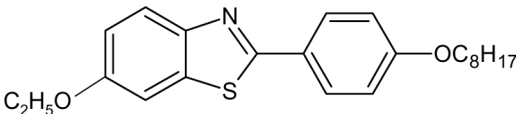
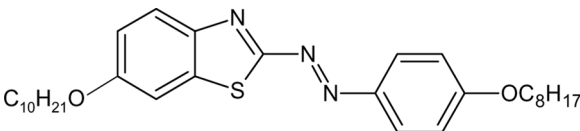


FIGURE 6 XRD patterns of **100-PBTH** and **120-PBTH** at different temperatures upon cooling from the isotropic phase.

Meanwhile, the additional azo linkage also tends to increase the transition temperatures and mesophase range of compound **A** when compared to **80-PBTH**. The increase in the mesophase range of compound **A** could have originated from (i) an increase in the length-to-breadth ratio of the molecule and (ii) an increase in the polarizability due to the extension of π -conjugation [33].

Structurally related compound **B** exhibited a smectic C phase instead of a nematic or smectic A phase. Upon comparison to **80-PBTH**,

TABLE 3 Transition Temperatures, Mesophase Range, and Molecular Structures of **8O-PBTH**, **A**, **B**, and **C**

		8O-PBTH	
		Compound A	
		Compound B	
		Compound C	
Compound	Transition temperatures (°C)	Mesophase range (°C)	
		Sm	N
8O-PBTH	Cr (SmA 74.8)* 75.5 I	–	–
A	Cr 94 N 136 I	–	42
B	Cr 106 SmC 134 I	28	–
C	Cr 70.7 SmC 95.0 N 123.8 I	24.3	28.8

(*) Monotropic value.

it can be rationalized that the presence of the ethoxyl substituent at the sixth position of the benzothiazole ring promoted the formation of the smectic C phase in compound **B**. The ethoxyl group in compound **B** favoured the intermolecular interaction that gave rise to a tilted arrangement of the molecules in the smectic layers. The similar pattern can also be inferred by comparing the molecular structures of compound **A** and **C**. It is clearly observed that as the length of the alkoxy chain at the sixth position of the benzothiazole ring increases, the molecules favour the tilted SmC phase.

CONCLUSION

In this article, we have reported the synthesis and mesomorphic properties of a homologues series of 2-(4-alkyloxyphenyl)benzothiazoles.

The n-octyloxy to n-hexadecyloxy derivatives exhibited a monotropic smectic A phase. The remaining members were non-mesomorphic. Comparison of the present series with other structurally related compounds revealed that transition temperatures and mesophase stability were greatly affected by the linking (terminal and centre) groups. The presence of the azo linkage disrupts the lamellar packing hence generating the nematic phase. The study also revealed that the methoxyl group at the sixth position of the benzothiazole ring stabilized the nematic phase whereas the ethoxyl group or a longer alkoxy chain at the sixth position of the benzothiazole ring will stabilize the smectic C phase.

ACKNOWLEDGMENTS

Author S. T. Ha would like to thank Universiti Tunku Abdul Rahman (UTAR) for the research facilities and the Malaysia Toray Science Foundation (UTAR Vote No. 4359/000) for funding this project. T. M. Koh would like to acknowledge UTAR for the award of the research assistantship. The partial financial support from MOSTI via the eSciencefund (Project No. 03-01-05-SF0366) is also essential to make this project complete. The powder XRD measurements are supported by beamline BL17A (charged by Dr. Jey-Jau Lee) of the National Synchrotron Radiation Research Center, Taiwan.

REFERENCES

- [1] Collings, P. J., & Hird, M. (1998). *Introduction to Liquid Crystals*, Taylor & Francis Ltd.: London, UK.
- [2] Seed, A. (2007). *Chem. Soc. Rev.*, 36, 2046.
- [3] Parra, M., Alderete, J., Zuniga, C., Gallardo, H., Hindalgo, P., Veragara, J., & Hernandez, S. (2001). *Liq. Cryst.*, 28, 1659.
- [4] Parra, M. L., Saavedra, C. G., Hildago, P. I., & Elgueta, E. Y. (2008). *Liq. Cryst.*, 35(1), 55.
- [5] Lai, L. L., Wang, C. H., Hsien, W. P., & Lin, H. C. (1996). *Mol. Cryst. Liq. Cryst.*, 287, 177.
- [6] Bartulin, J., Zuniga, C., Ramirez, A., Muller, H., & Taylor, T. R. (1990). *Mol. Cryst. Liq. Cryst.*, 185, 131.
- [7] Karamysheva, L. A., Kovshev, E. L., Pavluchenko, A. I., Roitman, K. V., Titov, V. V., Torgova, S. I., & Grebenkin, M. F. (1981). *Mol. Cryst. Liq. Cryst.*, 67, 254.
- [8] Karda, D., Mieczkowski, J., Pociecha, D., Szydloska, J., & Gorcecka, E. (2001). *J. Mater. Chem.*, 11, 741.
- [9] Champa, R. A. (1973). *Mol. Cryst. Liq. Cryst.*, 19, 23.
- [10] Dave, J. S., & Menon, M. (2000). *Bull. Mater. Sci.*, 23, 237.
- [11] Milkhalava, M. A. (2003). *Chem. Heterocycl. Comp.*, 39, 1032.
- [12] Thaker, B. T., Patel, P., Vansadia, A. D., & Patel, H. G. (2007). *Mol. Cryst. Liq. Cryst.*, 466, 13.

- [13] Parra, M., Vergara, J., Zuniga, C., Soto, E., Sierra, T., & Serrano, J. L. (2005). *Liq. Cryst.*, 32(4), 457.
- [14] Parra, M., Alderete, J., Zuniga, C., Gallardo, H., Hildago, P., Veragara, J., & Hernandez, S. (2000). *Liq. Cryst.*, 27, 995.
- [15] Funahashi, M., & Hanna, J. I. (1996). *Jpn J. Appl. Phys.*, 35, L703.
- [16] Funahashi, M., & Hanna, J. I. (1997). *Phys. Rev. Lett.*, 78, 2184.
- [17] Funahashi, M., & Hanna, J. I. (1997). *Mol. Cryst. Liq. Cryst.*, 304, 429.
- [18] Pavluchenko, A. I., Smirnova, N. I., Titov, V. V., Kovahev, E. I., & Djumaev, K. M. (1976). *Mol. Cryst. Liq. Cryst.*, 37, 35.
- [19] Belmar, J., Parra, M., Zuniga, C., Perez, C., & Munoz, C. (1999). *Liq. Cryst.*, 26, 389.
- [20] Prajapati, A. K., & Bonde, N. L. (2006). *J. Chem. Sci.*, 118(2), 203.
- [21] Demus, D., & Richter, L. (1978). *Textures of Liquid Crystals*, Verlag Chemie: New York.
- [22] Dierking, I. (2003). *Textures of Liquid Crystals*, Wiley-VCH: Weinheim.
- [23] Toba, M., Takeoka, Y., Rikukawa, W., & Sanui, K. (2005). *Synth. Met.*, 152, 197–200.
- [24] Prajapati, A. K., Vora, R. A., & Pandya, H. M. (2001). *Mol. Cryst. Liq. Cryst.*, 369, 37–46.
- [25] Vicini, P., Geronikaki, A., Incerti, M., Busonera, M., Poni, G., Cabras, C. A., & Colla, P. L. (2003). *Bioorg. & Med. Chem.*, 11, 4785.
- [26] Gray, G. W. (1962). *Molecular Structure and Properties of Liquid Crystals*, Academic Press: London.
- [27] Liu, C.-T. (1981). *Mol. Cryst. Liq. Cryst.*, 74, 25.
- [28] Kumar, S. (2001). *Liquid Crystals: Experimental Study of Physical Properties and Phase Transitions*, Cambridge University Press: U.K.
- [29] Wang, Y., Zhang, B. Y., He, X. Z., Wang, J. W. (2007). *Colloid Polym. Sci.*, 285, 1077.
- [30] Meng, F. B., Gao, Y. M., Lian, J., Zhang, B. Y., & Zhang, F. Z. (2008). *Colloid Polym. Sci.*, 286, 873.
- [31] Xiao, W., Zhang, B., & Cong, Y. (2008). *Colloid Polym. Sci.*, 286, 267.
- [32] Aldred, M. P., Vlachos, P., Dong, D., Kitney, S. P., Tsoi, W. C., O'Neill, M., & Kelly, S. M. (2005). *Liq. Cryst.*, 32(8), 951.
- [33] Vieira, A. A., Cristiano, R., Bortoluzzi, A. J., & Gallardo, H. (2007). *J. Mol. Struct.*, 875, 364.